PROCEEDINGS OF SCIENCE

Measurements of the CP structure of Higgs boson couplings with the ATLAS detector

Marina Kholodenko[a,b] **on behalf of the ATLAS Collaboration**

[a] *Laboratory of Instrumentation and Experimental Particle Physics, Av. Prof. Gama Pinto, n.2, Lisboa, Portugal*

[b] *Departamento de Física, Instituto Superior Técnico, Universidade de Lisboa, Av. Rovisco Pais 1, 1049-001 Lisboa, Portugal*

E-mail: marina.kholodenko@cern.ch

The Standard Model predicts the Higgs boson to be a CP-even scalar, but CP-odd contributions to its interactions with vector bosons and quarks are not yet strongly constrained. Various Higgs boson production and decay processes provide valuable tools to investigate the CP nature of these interactions. This talk presents the most recent measurements of the CP properties of Higgs boson interactions with vector bosons, performed by the ATLAS experiment at LHC using proton-proton collision data collected at $\sqrt{s}$ = 13 TeV. These results offer important constraints on possible CP-violating effects, advancing our understanding of Higgs boson dynamics.

The European Physical Society Conference on High Energy Physics (EPS-HEP2025)
7-11 July 2025
Marseille, France

 ISSN 1824-8039 . Published by SISSA Medialab.

https://pos.sissa.it/

PoS(EPS-HEP2025)358

1. Introduction

The origin of the observed baryon asymmetry in the universe is one of the fundamental open questions in our current understanding of particle physics. In 1967, Sakharov proposed three necessary conditions [1] to explain the generation of the baryon asymmetry. Among them, the charge-parity (CP) symmetry violation is required to create an excess of baryons over antibaryons in the early universe. But the sources of CP violation in the Standard Model (SM), which come from the complex phase in the quark mixing matrix [2], are insufficient to explain the observed matter antimatter imbalance.

While the SM Higgs boson is a scalar particle which is even under CP transformations, CP-violating interactions are not yet excluded by current experimental data. Therefore, measurements of the CP structure of the Higgs boson interactions with SM particles can be performed to search for sources of CP violation. Any deviation from the SM predictions would be a sign of physics beyond the SM (BSM).

This text presents five recent searches for CP violation in the Higgs boson interactions with vector bosons performed by the ATLAS collaboration. They use proton-proton collision data collected by the ATLAS detector [3] at the Large Hadron Collider (LHC) in Run 2 (2015-2018), corresponding to an integrated luminosity of $139 - 140$ fb^{-1} at a center-of-mass energy of 13 TeV.

2. Theoretical framework

In order to search for a clear sign of physics beyond the SM in a model independent way, the effective field theory (EFT) framework [4] is used. In this approach, the BSM contributions to the SM tensor structure are parameterised by higher dimensional operators ${O_i}^{(d)}$ of dimension d, and combined with the SM Lagrangian $\mathcal{L}_{SM}$ to form an EFT Lagrangian:

$$\mathcal{L}_{\text{SMEFT}} = \mathcal{L}_{\text{SM}} + \sum_{d>4} \sum_{i} \frac{c_i O_i^{(d)}}{\Lambda^{(d-4)}} \tag{1}$$

with dimension $d > 4$, Λ the scale of the new physics, and c_i the Wilson coefficients describing the strength of the new interactions. In the analyses presented below only operators of dimension-6 are considered and the Λ scale is set to 1 TeV. Operators with odd dimension imply lepton and baryon number violation, and are therefore ignored. Higher dimension operators such as dimension-8 are also not considered, since they are suppressed by an additional factor Λ^2. From this formulation of the effective Lagrangian it is possible to obtain a complete set of independent operators. However, there is no unique way to do it. Among the most used EFT operator bases are the HISZ, Warsaw and Higgs bases [5]. The total cross-section, which is proportional to the squared matrix element ($\mathscr{M}$) can be written as

$$|\mathscr{M}|^2 = |\mathscr{M}_{\text{SM}}|^2 + 2c_i \,\text{Re}\big(\mathscr{M}^*_{\text{SM}}\, \mathscr{M}_{\text{CP-odd}}\big) + c_i^2 |\mathscr{M}_{\text{CP-odd}}|^2. \tag{2}$$

The first term represents the SM contribution. The second term (interference term), which arises from the interference between SM and BSM, is *CP*-odd when only CP-odd operators are considered. This term introduces a new source of *CP* violation in Higgs boson couplings, and is parameterised

by the Wilson coefficient c_i. The third term (quadratic term) describes a *CP*-even BSM contribution parameterised by c_i^2. The interference term only affects *CP*-odd observables and does not contribute to *CP*-even observables.

Observables sensitive to CP-odd effects are used to probe CP-violating BSM operators. The so-called optimal observable (OO) is used as a discriminant in three searches presented here. It is defined by the ratio of the interference term in the matrix element (ME) to the SM contribution:

$$OO = \frac{2\Re(\mathcal{M}^*_{\text{SM}}\mathcal{M}_{\text{CP-odd}})}{|\mathcal{M}_{\text{SM}}|^2}.$$

The optimal observables are CP-odd by construction, implying a symmetric distribution with a vanishing mean in the absence of CP violation. Any asymmetry observed in the distribution of the optimal observables would be direct evidence for CP-violation. Other analyses may use angular observables, as presented in section 3.3 and 3.4.

3. Results

3.1 Test of CP-invariance of the Higgs boson in vector-boson fusion production and in its decay into four leptons

This analysis searches for a visible CP-odd effect in vector-boson fusion (VBF) Higgs production and the $H \to ZZ^* \to 4l$ decay by employing optimal observables [6]. There are three dimension-6 operators with BSM CP-odd couplings in the SMEFT Lagrangian that can contribute to VBF production or the $H \to ZZ^* \to 4l$ decay, each associated with a Wilson coefficient considered in the Warsaw basis $c_{H\widetilde{W}}$, $c_{H\widetilde{W}B}$, $c_{H\widetilde{B}}$, Higgs basis $\widetilde{c}_{zz}$, $\widetilde{c}_{z\gamma}$, $\widetilde{c}_{\gamma\gamma}$ and HISZ basis $\widetilde{d}$. The parameter $\widetilde{d}$ is related to the Warsaw-basis couplings by the parameterisation $c_{H\widetilde{W}} = c_{H\widetilde{B}} = \frac{\Lambda^2}{v^2}\widetilde{d}$, where v is the Higgs boson vacuum expectation value. In the Higgs basis, it is equivalent to the direction $\widetilde{c}_{z\gamma} = 0$, $\widetilde{c}_{\gamma\gamma} = \sin^2\theta_W \cos^2\theta_W \widetilde{c}_{zz}$, where θ_W is the Weinberg angle. Two types of optimal observables are considered. Production-level optimal observables reflect the VBF production vertex, not considering the Higgs boson decay, and decay-level optimal observables that focus only on the decay.

This measurement targets CP-violating effects on the optimal-observable shapes and is optimized to be insensitive to any potential CP-even signature of BSM physics, which would only affect event rates. The event rates predicted by the signal model are not used in the fit, and only the changes in the shapes of the optimal-observable distributions as a function of the BSM couplings are exploited. Three different types of fits are performed: decay-only, production-only, and combined.

Overall there is good agreement between data and the SM expectation in OO distributions. All the mean values of OO distributions are compatible with zero, indicating that the data exhibit no measurable asymmetry. In absence of positive evidence for BSM physics, 68% and 95% confidence intervals on the CP-odd couplings are extracted with the profile likelihood ratio statistical test, using the negative-log likelihood test statistic. Only one Wilson coefficient is fitted at a time while all others are set to zero. Both interference and quadratic and interference terms only are considered, with quadratic term having a negligible impact on the limits. Limits are set on relevant EFT Wilson coefficients in both the Warsaw and Higgs basis and on the value of the $\widetilde{d}$ parameter in the HISZ

basis. No significant deviations from SM expectations are found in the search. The 95% CL intervals are $[-0.81, 0.54]$ for $c_{H\widetilde{W}}$ and $[-0.026, 0.025]$ for $\widetilde{d}$.

3.2 Test of CP-invariance in Higgs Boson in vector-boson fusion production using the $H \to \gamma\gamma$ channel

The next analysis presented here probes the CP-invariance in VBF Higgs Boson production with Higgs bosons decaying to two photons, $H \to \gamma\gamma$ [7]. This study adopts the optimal observable to test the CP-structure of Higgs boson couplings to electroweak bosons in VBF production.

The signal yield is extracted via a combined unbinned maximum-likelihood estimation applied to the $m_{\gamma\gamma}$ distribution of observed data in each OO bin. The confidence intervals on the parameters $\widetilde{d}$ and $c_{H\widetilde{W}}$ are obtained using negative-log likelihood test statistic. The analysis exploits only the shape of the distribution of the optimal observable, and ignores the potential dependence of the inclusive cross section.

The 95% CL limits on the dimension-6 Wilson coefficients are $[-0.032, 0.059]$ for $\widetilde{d}$ and $[-0.53, 1.02]$ for $c_{H\widetilde{W}}$ using interference term only and $[-0.034, 0.071]$ for $\widetilde{d}$ and $[-0.55, 1.07]$ for $c_{H\widetilde{W}}$ using interference plus quadratic terms. The results are compatible with the SM and the precision is limited by the statistical uncertainty of the data.

3.3 Measurements of Higgs boson production via gluon-gluon fusion and vector-boson fusion using $H \to WW^* \to \ell\nu\ell\nu$ decays

This analysis presents a search of CP-violation in Higgs boson production via gluon–gluon fusion (ggF) and VBF using $H \to WW^* \to \ell\nu\ell\nu$ decays [8]. Different and same flavour combinations of the final-state lepton pair are considered. The signal strengths, defined as the production cross-sections times the $H \to WW^*$ branching fraction relative to their SM prediction, are measured in an Simplified Template Cross-Section STXS scheme [9] (Stage 1.2 [10, 11]), which splits the production modes of the simulated Higgs boson into experimentally accessible exclusive kinematic fiducial regions or 'categories' that are relevant for theory interpretations. STXS categorization is based on the number of jets, the Higgs boson transverse momentum, and, for VBF production, the invariant mass of the two highest-p_T jets. For CP violation studies, the STXS categories are further divided in bins of the CP-sensitive variable: the azimuthal angular difference between the two leading jets, ordered by rapidity $\Delta\phi^{\pm}_{jj}$. The selected events are split in four bins: $[-\pi, -\pi/2)$, $[-\pi/2, 0)$, $[0, +\pi/2)$, $[+\pi/2, +\pi)$ of the angular variable. The measured signal strengths are used to constrain the impacts of two CP-odd effective operators (with Wilson coefficients $c_{H\widetilde{W}}$, $c_{H\widetilde{G}}$) and their CP-even counterparts (with Wilson coefficients c_{HW}, c_{HG}) on Higgs boson production and decay.

A deep neural network (NN) is trained to identify the signal topology targeted in each signal region, and the output of the deep NN is used as the discriminating variable in the fit. CP violation will manifest as an asymmetry of the $\Delta\phi^{\pm}_{jj}$ distribution. To ensure that only shape information is used to constrain CP-violating effects, and therefore provide a genuine test of CP violation, each STXS category is scaled by a 'signal normalisation factor', that coherently scales the normalisation of the same category across all the $\Delta\phi^{\pm}_{jj}$ bins and is treated as a nuisance parameter. Only the interference between the SM and BSM operator are considered in this measurement. All four

Wilson coefficients are obtained from a simultaneous fit to data, the results of which are shown in Figure 1a. Each Wilson coefficient is consistent with the SM expectation within its 95% CL interval. The correlations between different observed values of the Wilson coefficients are all less than 5% in absolute value, as can be seen in Figure 1b. All measurements are compatible with the SM predictions.

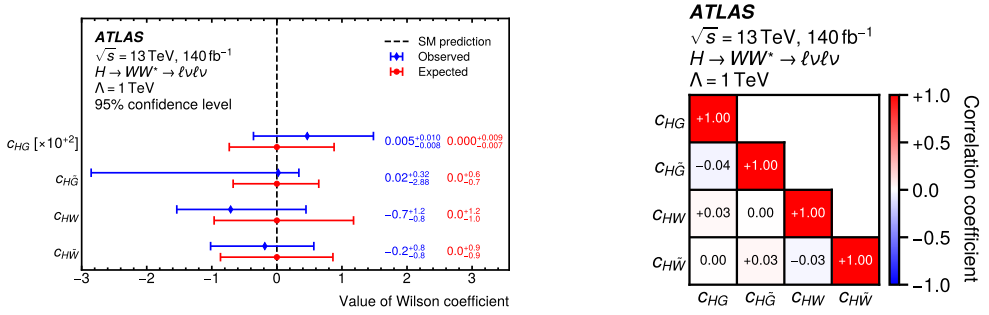

(a) **(b)**

Figure 1: (a) Best-fit values and uncertainties and (b) correlations for the Wilson coefficients considered by the SMEFT interpretation of the STXS measurements in $H \to WW^* \to \ell\nu\ell\nu$. The best-fit values and uncertainties for the observed (expected) results are given by the leftmost (rightmost) numbers on each line. The error bars and quoted errors correspond to the total 95% CL interval in each Wilson coefficient [8].

3.4 Search for CP violating effects in HWW vertex in the WH production channel

This analysis is a search for CP violation in the interaction between the Higgs and W bosons, via WH production [12]. This production channel allows for constraining the HWW vertex separately from the HZZ vertex, which is not the case for the searches via VBF production. A CP-sensitive analysis of WH production with Higgs boson decays into bottom quarks $WH, H \to b\bar{b}$ is performed, based on the measurement of $VH, H \to b\bar{b}$ described in Ref. [13]. Out of the five dimension-6 operators which affect the $pp \to WH$ process, there is only one CP-odd operator, $O_{H\widetilde{W}}$ with corresponding Wilson coefficient $c_{H\widetilde{W}}$. The measurement presented in this note is performed using a modified version of angular observable $\cos\delta^+$ introduced in Ref. [14], designed to retain sensitivity to the CP-odd behavior introduced by the interference between the SM and the SMEFT $O_{H\widetilde{W}}$ term in the Lagrangian. It is defined as follows:

$$Q_\ell \cos\delta^+ = Q_\ell \frac{\mathbf{p}_\ell^{(W)} \cdot (\mathbf{p}_H \times \mathbf{p}_W)}{|\mathbf{p}_\ell^{(W)}| \cdot |\mathbf{p}_H \times \mathbf{p}_W|}, \tag{3}$$

where Q_ℓ is the lepton charge, $\mathbf{p}_\ell^{(W)}$ is the momentum of the charged lepton in the W boson rest frame and $\mathbf{p}_W$, $\mathbf{p}_H$ are the momenta of the W and Higgs bosons, respectively, in the laboratory frame. Fiducial cross section measurements are performed using an extended version of the STXS framework, stage 1.2. STXS regions are defined using the *truth* record of the event, classifying the events in a two dimensional grid based on the transverse momentum of the W boson and the angular observable $Q_\ell \cos\delta^+$. The cross section measurements obtained are then interpreted in terms of constraints on the CP-odd Wilson coefficient $c_{H\widetilde{W}}$, by considering only the linear term in

the SMEFT expression of the $pp \to WH$ cross-section. The interpretation relies on expressing the truth-level cross-section in each STXS bin as a function of $c_{H\widetilde{W}}$ using SMEFTsim 3.0.

The measured signal strength, i.e. the cross section times branching fraction normalised to the SM expectation, for each one of the STXS regions is shown in Figure 2a. The experimental precision is generally dominated by the statistical uncertainty, with the exception of the first p_T^W bin where the systematic uncertainties are larger. Overall, the results are in agreement with the SM expectations, with no clear pattern distinguishing the positive or negative bins of the angular observable $Q_\ell \cos\delta^+$. A fit to the STXS regions is performed with 5 parameters of interest: the CP-odd Wilson coefficient $c_{H\widetilde{W}}$ and the signal normalisation factors in each p_T^W bin (correlated across $Q_\ell \cos\delta^+$ regions). This configuration ensures sensitivity to CP-odd effects by explicitly factorizing out the effect on the signal scale. The resulting observed and expected negative profile likelihood scans as a function of $c_{H\widetilde{W}}$ are shown in Figure 2b. The observed 95% CL interval on the Wilson coefficient $c_{H\widetilde{W}}$ is [-0.54, 0.74] . These results represent the first measurements of the CP-odd operator in WH production channel.

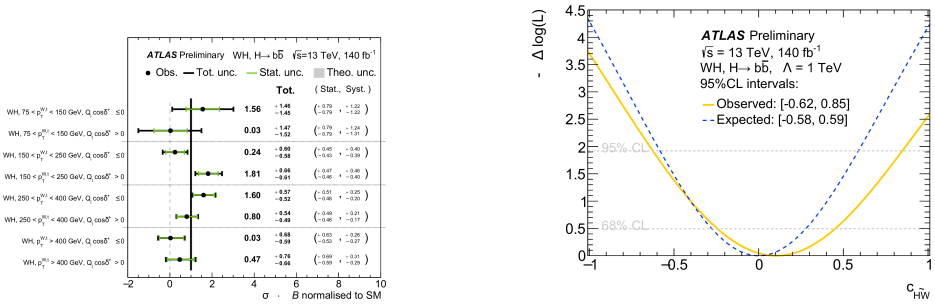

(a) **(b)**

Figure 2: (a) Measured WH production cross sections times the $W \to l\nu$ and the $H \to b\bar{b}$ branching ratios. The measured signal significance with its corresponding uncertainty is shown for all regions. (b) Expected and observed scans of the likelihoods for the CP-odd Wilson coefficient $c_{H\widetilde{W}}$ using a linear-only parameterization. All other Wilson coefficients are set to 0 [12].

3.5 Probing the Higgs boson CP properties in vector-boson fusion production in the $H \to \tau^+\tau^-$ channel

In this analysis, a search for CP violation in the VBF production vertex of the Higgs boson is performed in the $H \to \tau\tau$ decay mode using an optimal observable [15]. Three combinations of τ-lepton decays are considered: fully hadronic, where both τ-leptons decay to hadrons and a neutrino; semileptonic, where one decays hadronically and the other to $l\nu\bar{\nu}$, $l = e, \mu$; and leptonic, where one decays to $e\nu\bar{\nu}$ and the other to $\mu\nu\bar{\nu}$. Same-flavour leptonic decays are rejected due to the large contribution from $Z \to e^+e^-$ and $Z \to \mu^+\mu^-$ backgrounds. To construct an enriched signal region, a multivariate classifier based on NN is used. For each channel, a separate NN is optimised to best exploit the different compositions and features of the channels. Each of the signal regions are binned in the OO. The binning of the signal regions in the three channels is optimised to have an equal number of expected SM signal events in each bin. All three channels have a total of 10 bins. For each signal region, one control region is defined to constrain the $Z \to \tau\tau$ background.

The normalisation of the signal is added as a common free floating normalisation factor. In this way, the analysis is not sensitive to overall changes in the total cross-section that might be due to additional CP-even terms, but only considers differences in shapes of OO, and is therefore only sensitive to the interference term of the EFT model.

The statistical analysis is performed using a binned maximum-likelihood fit. The sensitivity to the CP-odd coupling (either in the HISZ or the Warsaw basis), is estimated by doing a negative-log likelihood scan. The negative-log likelihood is computed for different hypotheses of the parameter of interest, using signal template samples constructed by reweighting the SM VBF Higgs signal. Figure 3a shows the expected and observed 95% CL intervals for $\widetilde{d}$ and $c_{H\widetilde{W}}$ considering both interference and quadratic terms, as well as interference term only. For all the interpretations, the difference of adding the quadratic term is small, relaxing the limits by about 10%. In all cases, the CP-violating Wilson coefficients are compatible with zero.

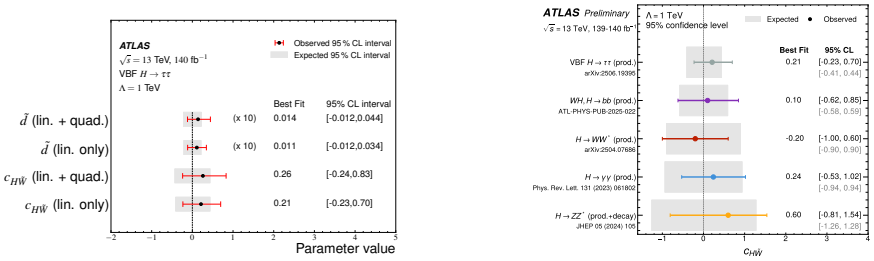

(a) **(b)**

Figure 3: (a) Expected and observed best fit values and 95% CL intervals for all the CP-violating Wilson coefficients considered in the $H \to \tau\tau$ analysis [15]. (b) Comparison of results for the expected and observed measurements of the CP-odd Wilson coefficient $c_{H\widetilde{W}}$ for five presented measurements [16].

4. Conclusion

This paper presents five recent searches of CP violation in Higgs boson interaction with electroweak bosons with ATLAS detector at LHC using the full Run 2 dataset. No statistically significant deviation relative to the Standard Model prediction of a CP-even coupling between the Higgs boson and vector bosons is observed. All the results are interpreted using EFT framework. A comparison of the results for the expected and observed measurements of the CP-odd Wilson coefficient $c_{H\widetilde{W}}$ is presented on Figure 3b for the five measurements discussed above. All results are obtained via a linear-only interpretation, with the exception of the ATLAS $H \to ZZ^* \to 4l$ result, where the quadratic term is also considered but has been shown to have a negligible impact on the limits. The $H \to WW^*$ result is obtained via a simultaneous fit to Wilson coefficients $c_{H\widetilde{W}}$, c_{HW}, $c_{H\widetilde{G}}$ and c_{HG}, but the correlations between their different observed values are small. The data and 95% CL bars show the observed values with statistical and systematic uncertainties, and the grey bands centered at 0 show the expected 95% CL intervals. The best fit values and 95% CL observed (expected) limits are also explicitly listed on the right-most side of the plot in black (gray).

Acknowledgments

Marina Kholodenko is financed by Portuguese national funds through FCT, Fundação para a Ciência e a Tecnologia, I.P., within the scope of the project 2024.00227.CERN and through a PhD grant.

References

[1] A.D. Sakharov, *Violation of CP invariance, C asymmetry, and baryon asymmetry of the universe*, *Soviet Physics Uspekhi* **34** (1991) 392.

[2] A. Hocker and Z. Ligeti, *CP violation and the CKM matrix*, *Ann. Rev. Nucl. Part. Sci.* **56** (2006) 501 [hep-ph/0605217].

[3] ATLAS Collaboration, *The ATLAS Experiment at the CERN Large Hadron Collider*, *JINST* **3** (2008) S08003.

[4] I. Brivio and M. Trott, *The standard model as an effective field theory*, *Physics Reports* **793** (2019) 1–98.

[5] G. Isidori, F. Wilsch and D. Wyler, *The standard model effective field theory at work*, *Rev. Mod. Phys.* **96** (2024) 015006 [2303.16922].

[6] ATLAS Collaboration, *Test of CP-invariance of the Higgs boson in vector-boson fusion production and in its decay into four leptons*, *JHEP* **05** (2024) 105 [2304.09612].

[7] ATLAS Collaboration, *Test of CP Invariance in Higgs Boson Vector-Boson-Fusion Production Using the $H\to\gamma\gamma$ Channel with the ATLAS Detector*, *Phys. Rev. Lett.* **131** (2023) 061802 [2208.02338].

[8] ATLAS Collaboration, *Measurements of Higgs boson production via gluon-gluon fusion and vector-boson fusion using $H \to WW^* \to \ell\nu\ell\nu$ decays in pp collisions with the ATLAS detector and their effective field theory interpretations*, 2504.07686.

[9] LHC Higgs Cross Section Working Group collaboration, *Handbook of LHC Higgs Cross Sections: 4. Deciphering the Nature of the Higgs Sector*, 1610.07922.

[10] J.R.A. et al., *Simplified template cross sections - stage 1.1*, 1605.04692.

[11] N. Berger et al.,, *Les Houches 2015: Physics at TeV Colliders Standard Model Working Group Report*, 1906.02754.

[12] ATLAS Collaboration, "Search for CP violation in WH production in 13 TeV pp collisions with the ATLAS detector." ATL-PHYS-PUB-2025-022, 2025.

[13] ATLAS Collaboration, *Measurements of WH and ZH production with Higgs boson decays into bottom quarks and direct constraints on the charm Yukawa coupling in 13 TeV pp collisions with the ATLAS detector*, *JHEP* **04** (2025) 075 [2410.19611].

[14] R.M. Godbole, D.J. Miller, K.A. Mohan and C.D. White, *Jet substructure and probes of CP violation in Vh production*, *Journal of High Energy Physics* **2015** (2015) 103 [1409.5449].

[15] ATLAS Collaboration, *Probing the Higgs boson CP properties in vector-boson fusion production in the $H \to \tau^+\tau^-$ channel with the ATLAS detector*, 2506.19395.

[16] ATLAS Collaboration, "Summary of constraints on CP-odd contributions to the HVV coupling." ATL-PHYS-PUB-2025-031, 2025.